Role of the structure and reactivity of Cu and Ag surfaces in the formation of a 2D metal-hexahydroxytriphenylene network

Alain Rochefort,*,† Loranne Vernisse,‡ Ana Cristina Gómez-Herrero,¶ Carlos Sánchez-Sánchez,§ José Angel Martín-Gago,§ Frédéric Chérioux,‖ Sylvain Clair,⊥ Johann Coraux,¶ and José I. Martínez§

†Département de génie physique, Polytechnique Montréal, Montréal (Qué), H3C 3A7, Canada.

‡Institut P', UPR 3346, Département de Physique et Mécanique des Matériaux, CNRS – Université de Poitiers – ENSMA, Poitiers, France.

¶Université Grenoble Alpes, CNRS, Grenoble INP, Institut NÉEL, F-38000 Grenoble, France.

§ESISNA Group, Institute of Materials Science of Madrid (ICMM-CSIC), C/Sor Juana Inés de la Cruz 3, E-28049 Madrid, Spain.

‖Université Bourgogne Franche-Comté, FEMTO-ST, CNRS, UFC, 15B Avenue des Montboucons, F-25030 Besançon Cedex, France

⊥Aix Marseille Univ, Université de Toulon, CNRS, IM2NP, Marseille, France.

E-mail: alain.rochefort@polymtl.ca

1

Abstract

We have investigated the role played by the atomic structure and reactivity of the supporting Ag(111) and Cu(111) surfaces on the formation of 2D metal-organic networks (2D-MON) involving metal adatom clusters spawned by these two surfaces. While the hexahydroxytriphenylene (HHTP) molecule forms complexes with Ag_3 and Cu_3 adatom clusters on respectively, the Ag(111) and Cu(111) surfaces, extended order is only observed in the 2D-MON on Ag(111). By combining scanning tunneling microscopy (STM) measurements, density functional theory (DFT) calculations and microscopy image simulations, we show that the formation of Ag-HHTP metal-organic complexes is structurally compatible with a periodic arrangement of HHTP on the Ag(111) surface. In contrast, on Cu(111), tightly-bonded and localized Cu-HHTP motifs are stabilized by the interaction of Cu ad-clusters with HHTP. However, they cannot match the surface structure of Cu(111) to form an extended 2D-MON. We observed that the formation of large 2D-MON domains on a metallic surface is only possible when the periodicity of the adsorbed surface assembly is weakly perturbed by the addition of metal ad-clusters that reinforced the bonding.

Introduction

Understanding the physical and chemical processes in which local interactions lead to ordered structures is of particular relevance to the realization of molecular architectures on surfaces. By taking advantage of the directional bonding of specific molecule-molecule and/or molecule-surface interactions, and by choosing the appropriate symmetry for the molecules and the electronic properties of the surfaces, remarkable 2D extended structures have been achieved.[1–4] These structures are mainly observed by scanning probe microscopies under ultra-high vacuum (UHV) conditions in order to reach submolecular resolution to unambiguously identify the designed-structures. Among all possibilities to create ordered structures on a surface, the complexation with metal atoms has been widely used.[5–12] In this case, the

formation of metal-organic networks, consisting in oxygen-bearing molecular units intercon-nected via metallic centers, has been widely explored at the surface of metals under UHV conditions.[13,14] The required metal atoms are provided either extrinsically, by on-surface metal evaporation, or intrinsically, by the metal surface itself. Noteworthy, in the latter case, the coordination mechanism is activated by the oxidation of the molecular precursor that takes place spontaneously in UHV due to the electronic properties of the supporting surface.

Starting from alcohols, such oxidation (or dehydrogenation reaction) is straightforward on copper surfaces,[15–18] but also partially occurs on silver[15,19–23] and gold surfaces.[24] A peculiar kind of alcohol, the hexahydroxytriphenylene (HHTP) molecule, has attracted much attention in this respect. Depending on the degree of oxidation (and of dehydrogenation), the molecule can find different applications and exhibit peculiar properties. The HHTP molecule is a model compound forming a variety of two- or three-dimensional metal organic frameworks (MOFs) in its semiquinoid form.[25–27] It has also been used to prepare 2D layered systems accommodating anions in a host-guest structure.[28] This precursor is thus particularly well-suited for creating surface-supported MOFs. The supramolecular self-assembly of HHTP and the related dehydrogenation reaction on metal single-crystal surfaces have been extensively studied.[18,19,29–32] Here, we show that metal-organic phases can form on the Ag(111) and Cu(111) surfaces, with different stability depending on the substrate nature and on the dehydrogenation level.

METHODS

Experimental details

2,3,6,7,10,11-hexahydroxytriphenylene (HHTP) molecules were purchased from TCI-Europe (95% purity). This compound was purified at the laboratory by repeated washing in organic solvents until a purity of >99% was reached, as checked with 1H and 13C NMR experiments.

Scanning tunneling microscopy experiments have been performed in two separate UHV systems both equipped with STM, one from SIGMA Surface Science operated at liquid nitrogen temperature (79 K), and the other at ambient temperature on a homemade STM, with base pressures in the 10^{-11}-10^{-10} mbar range. The Ag(111) and Cu(111) crystals were cleaned by repeated Ar^+ bombardment cycles at E = 600 eV and 800 eV, followed by annealing for one hour at around 650 K for Cu(111) and 800 K for Ag(111). This cleaning procedure was completed by STM measurements of the single-crystal samples. The HHTP molecules were evaporated on the samples kept at different temperatures from molybdenum crucibles heated to 500 K for Ag(111) and from homemade Ta pockets and quartz crucibles heated to 550 K for Cu(111). On Ag(111), large domains of the P2* structure were only obtained through deposition using low deposition rate (0.01 ML/min) on a hot substrate (473 K). On Cu(111), another preparation procedure (temperature treatment consisting in annealing molecules deposited at room temperature beforehand) was also tested, and is not further discussed below since it produces no significant difference in our STM observations. STM experiments were recorded in the constant current mode. Images were processed with the free softwares WSxM[33] and Gwyddion.[34]

Computational methodology

Density functional theory (DFT) calculations on gas phase complexes were carried out at T = 0 K with the NWChem[35] package, we used the generalized gradient approximation using the PBE0 functional[36] and we considered energy correction for the van der Waals interactions.[37] We used 6-31G** basis sets to describe all H, C, O and N atoms.

The structure and adsorption energy of non-dehydrogenated, partially-dehydrogenated and fully-dehydrogenated HHTP molecules on Cu(111) and Ag(111) were optimized by using the QUANTUM ESPRESSO plane-wave DFT code.[38] The Cu(111) and Ag(111) substrates were modelled by using four in-plane-periodic metal layers, the atomic positions in the two bottom ones being fixed during the structural relaxation process. The calculations take

into account an empirical efficient van der Waals (R^{-6}) correction (DFT+D2 method[37])
Electronic exchange and correlation effects were accounted for using the generalized gradient
approximation PBE functional.[39] Ultrasoft pseudopotentials were used to model the ion-
electron interaction within the H, C, O and Cu atoms.[40,41] The Brillouin zones were sampled
using optimal Monkhorst-Pack grids.[42] The one-electron wave-functions were expanded in
a basis of plane waves with 450 eV cutoff for the kinetic energy. Atomic relaxations were
performed until the maximum force acting on any atom was below 0.05 eV/Å.

Simulations of the STM images were performed within the Keldysh–Green function for-
malism[43] as implemented in the localized-basis set code FIREBALL,[44] where both sample
and tip contributions are explicitly treated. A simpler approach such as the Tersoff-Hamann
one[45] could provide reasonable representation of STM images, however in the present case,
the significant hybridization of the electronic orbitals of the metal and oxygen or carbon
atoms a priori calls for a more advanced treatment, such as the Keldysh-Green formalism.

Results and Discussion

Observations of molecular self-assemblies and metal-organic networks (MON).

The 2,3,6,7,10,11-hexahydroxytriphenylene molecule (HHTP) is made of a triphenylene core
surrounded by six hydroxyl groups. This molecule is a model compound to investigate
electron transfers induced between oxygen moieties attached to an aryl group (i.e. phenol)
and single cristal surfaces such as Cu(111) or Ag(111),[18,19] a process that is reminiscent of
those occurring, e.g., in biological cells[46,47] or energy applications.[27,48] We have analysed the
effect of this electron transfer onto the self-assembly of HHTP on Ag(111) and Cu(111) at
different temperatures of deposition.

Figure 1 compares STM images for an adsorption of HHTP at room temperature on
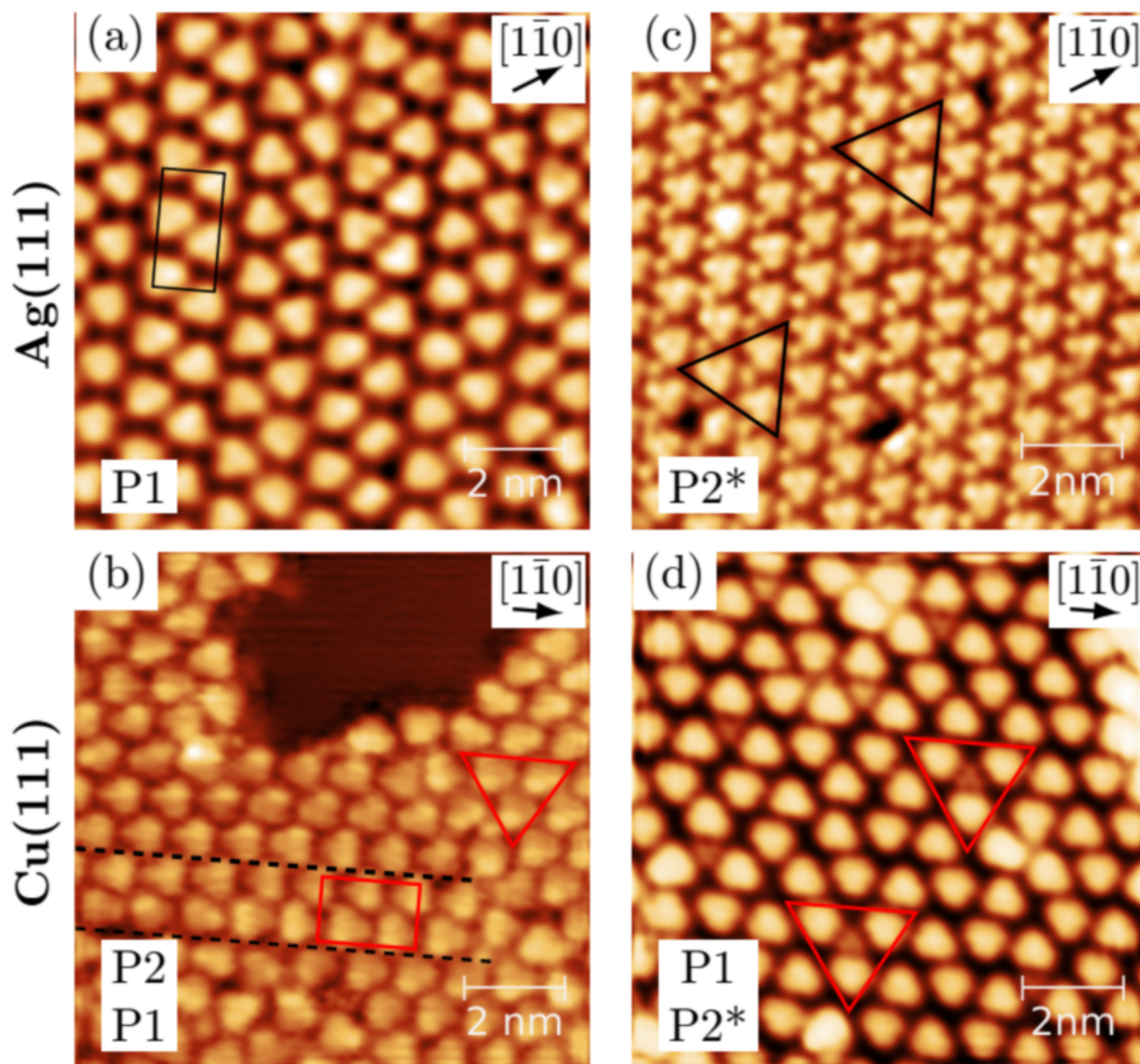Ag(111) and Cu(111) surfaces, to the images of the surface complexes formed at higher

Figure 1: STM images of HHTP assemblies for adsorption (a) at 293 K and (c) 473 K with low deposition rate (0.01 ML/min) on Ag(111), and (b) at 293 K and (d) 530 K on Cu(111) surfaces. P1 motif is identified by rectangles in (a) and (b), P2 is defined by triangle in (b), and P2* motif is identified by triangles in (c) and (d).

temperatures on the same substrates. On Ag(111), we observe a well-ordered 2D organization based on parallel saw-tooth nanolines constituted by paired triangular protrusions about 0.9 nm in size (see Fig. 1(a)). Each triangular bright protrusion is attributed to an individual HHTP molecule. On Cu(111) (Fig. 1(b)), similar triangular protrusions are observed, yet the degree of order is much lower than on Ag(111). We do observe local organisations in the form of parallel saw-tooth nanolines, resembling the P1 structure on Ag(111), but this organisation is limited to a few lines of protrusions at most (highlighted between black dotted lines in Figure 1(b)). These lines actually form boundaries between ordered patches, referred to as P2, where the bright protrusions assume a simpler, higher symmetry hexagonal periodicity (see red triangle highlighting a characteristic pattern in Figure 1(b)).

A deposition of HHTP at 473 K and 530 K on Ag(111) and Cu(111), respectively, produces different kinds of molecular organisations on the surfaces. The corresponding STM images are reported at a large scale in Figure S1 (see Supporting Information) and in a closer view in Figure 1(c)-(d). On Ag(111), the molecules form 2D islands of several 10 nm. They are constituted by periodic arrangements of three bright dots surrounding the triangular protrusions observed at room temperature described above. The repeating unit cell of this structure labelled P2* is composed of three molecules surrounding a bright dot (see black triangle in Fig. 1(c)). In contrast, STM images on Cu(111) show smaller domains (few 10 nm) composed of a molecular assembly with no long-range periodic arrangement. Characteristic features constituted by three molecules surrounding a dim feature made of three fainted dots are observed (highlighted by red triangles in Figure 1(d)). The small central features observed in Figure 1(c,d) (the bright dots on Ag(111) and the dim triple-dots on Cu(111)) are attributed to surface adatoms, Ag and Cu respectively. Such metal adatoms, involved in small clusters, were recently reported for thiolate on Cu(111) and Ag(111) surfaces,[49] and with other dehydrogenated oxygen-group-bearing molecules, dihydroxy-benzoquinone[15,50] and trimesic acid.[20]

Finally we briefly discuss the effect of annealing the samples, which could yield yet other

kinds of molecular phases. The temperature range that can be explored is however relatively limited. Above a certain temperature indeed, molecules will desorb from the surface and/or decompose. These processes are already prominent at 630 K on Cu(111),[18] and at 510 K on Ag(111). Before that, it is indeed possible to observe, on Ag(111) and in a very narrow temperature window (∼500 K), a honeycomb phase that has been coined P3 in previous works,[19] and on Cu(111) (610 K annealing), a kind of molecular arrangement featuring units with no resemblance to the original HHTP molecules (see figure S2 of Supporting Information), suggesting thermal decomposition of the molecules.

HHTP-metal clusters host-guest structures.

To clarify the origins of supramolecular organization and the role of metal clusters (Ag and Cu) in stabilizing the HHTP complexes, we have investigated the structure and stability of gas phase and adsorbed species with DFT calculations. We have shown previously that surface-assisted dehydrogenation occurs when HHTP molecules are deposited on Ag(111)[19] and Cu(111)[51] so we varied systematically the degree of dehydrogenation of the molecules in the calculations.

Figure 2(a) and Figure 2(b) show schematic views of the above-discussed P1 and P2 structures, respectively. P1 is relatively more dense and has a lower symmetry compared to P2. For the P2 structure, the nanoporosity is represented by the dashed circles. To form the P2* structure, the P2 structure can accommodate molecular guests such as anions.[28] Such porosity in P2 could also be filled by different Ag or Cu clusters that are chemically bonded to the HHTP units. According to the available surface area within a P2 trimer, we first considered the presence of planar metallic clusters built from 1, 2, 3 and 6 atoms, which can reasonably be nested inside the HHTP network without excessive cluttering. Figure 2(c) schematizes the results of DFT calculations about the equilibrium position of the metal clusters within metal-organic complexes. While a single metal atom or a dimer remains significantly bonded to dehydrogenated or pristine HHTP, this also introduces major

deformations of the network. Such deformations lead to the formation of highly asymmetric or twisted complexes. In fact, only Ag and Cu trimers give rise to highly symmetric and highly directional bonding in metal-HHTP complexes, with relatively small perturbation of the original porosity. Finally, although the 6 atoms cluster forms a symmetric and stable metal-organic complex, its presence among the P2 trimers can be only satisfied if the porosity increases. Then, in agreement with the STM observations of Fig.1(d), we will mainly consider the presence of metallic trimers within the HHTP network. The presence of Cu_3 clusters in surface networks has been reported several times in the literature, where their ability to form a three-fold type of bonding with organic ligands was noticed.[52,53] In previous works, it proved difficult to resolve, with STM, the inner structure of the clusters, yet with peculiar kinds of STM tip terminations (unfortunately obtained in a non reproducible way) three protrusions show up.[53] This is precisely what we observed on the Cu(111) surface, with the clusters appearing as three-fold features (Figure 1(d)). The formation of such three-atoms-clusters, Cu_3 and Ag_3, is further supported by our structural analysis summarized in Figure 2.

Geometry of HHTP-metal cluster networks on the metal surfaces.

The results from a detailed analysis of the different HHTP structures derived from STM measurements and DFT calculations are reported in Table 1. First, we note that the surface-free P1 structure is more compact than P2, because the distance between two HHTP molecules is systematically shorter in the P1 than in the P2 arrangement. In addition, the P2 structure is more sensitive to the dehydrogenation degree of the HHTP molecule than the P1 structure. Indeed, the average distance between two full hydrogenated HHTP molecule varies from 12.4 Å to 10.5 Å for fully dehydrogenated molecules ($\Delta d_{\text{mol-mol}}$ = -15 %) in the P2 arrangement. While, in the case of the P1 structure, the distance between two molecules is 9.8 Å in the two oxidation states. Finally, on the basis of the distance between non-dehydrogenated HHTP molecules in metal-free networks, both P1 and P2 structures would better fit on the
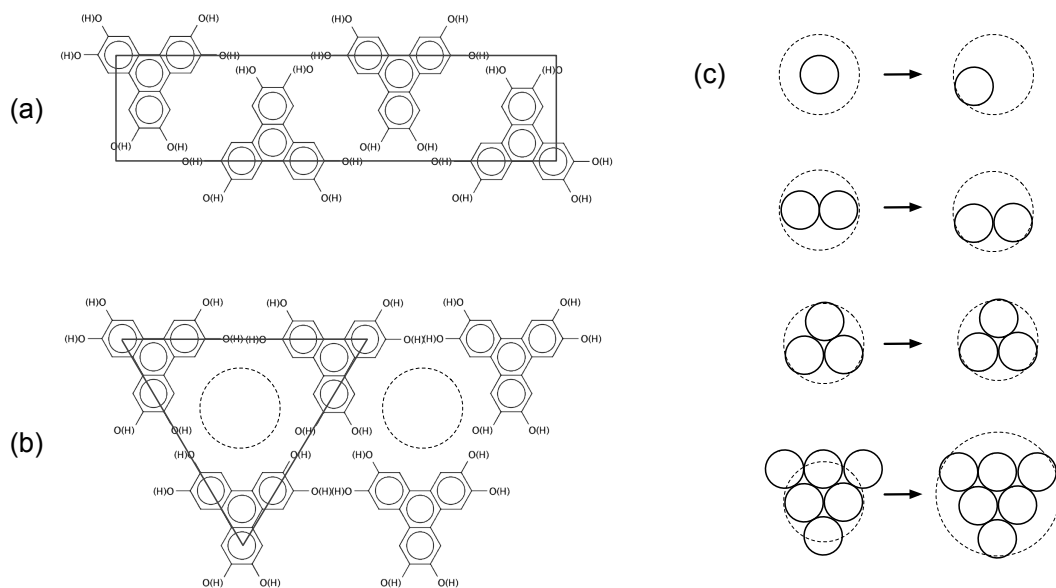
Figure 2: Molecular arrangement of HHTP molecules with (a) P1 and (b) P2 adsorbed structures. Depending of the deposition conditions, a partial or complete dehydrogenation of HHTP molecules (indicated by H in parenthesis) may result in the rotation of HHTP units while the overall arrangement is preserved. The porosity of P2, indicated by dashed circles, can be filled by metallic M_n cluster where $n = 1, 2, 3$ and 6 atoms. In (c), we show the starting geometry (left side) and stable (right side) complexes showing the position of the cluster within the porosity, or the expansion of the porosity when $n=6$.

Cu(111) surface where the periodicity along the $[1\bar{1}0]$ direction can be 10.1 Å (4×2.52 Å) or 12.6 (5×2.52 Å), than on Ag(111) where the closest periodicity is 11.6 Å (4×2.89 Å).

Table 1 also reveals that the structure of HHTP assemblies is weakly perturbed by the presence of Ag_3 on the Ag(111) surface with a distance always remaining in the range of 11.6-11.8 Å). In contrast, the HHTP self-assembly undergoes significant structural changes to accommodate the presence of Cu_3 on the Cu(111) surface (with a distance going from 13.1 to 11.3-11.6 Å). For example, fully dehydrogenated HHTP assembles into a compact P1 phase on the Cu(111) surface that agrees very well with the observed surface topography, while the Cu_3-HHTP system needs to arrange into a P2* structure where HHTP molecules are more weakly commensurate with the Cu(111). Such important structural transformation contributes to hinder the formation of large domains containing partially or fully dehydrogenated Cu_3-HHTP species.

Table 1: Distances ($d_{\text{mol-mol}}$) between HHTP molecules (in Å) where no, partial or total dehydrogenation have been considered. The interatomic distances of surface atoms are 2.89 Å[54] and 2.52 Å[55] for clean Ag(111) and Cu(111) single-crystals, respectively. P2* corresponds to the P2 structure including metal clusters. Freestanding gas-phase molecular systems without surfaces are included for comparison.

| system | surface | cluster | $d_{\text{mol-mol}}$ for various $(OH)_6$ dehydrogenation level | | | | | | | |
| | | | none (-0H) | | partial (-2H) | | partial (-3H) | | full (-6H) | |
			calc	exp	calc	exp	calc	exp	calc	exp
	gas-phase	-	9.8	-	9.3	-	9.3	-	9.8	-
P1	Ag(111)	-	11.6	11.5 ± 0.5[31]	11.6	-	-	-	-	-
	Cu(111)	-	-	-	-	-	-	10 ± 1	10.4[18]	9 ± 1
	gas-phase	-	12.4	-	11.4	-	11.4	-	10.5	-
P2	Ag(111)	-	-	-	-	-	11.6	11 ± 1[19]	11.6	-
	Cu(111)	-	-	-	13.1	-	13.0	13 ± 1[51]	-	-
	gas-phase	Ag$_3$	12.4	-	11.5	-	12.5	-	12.4	-
	gas-phase	Cu$_3$	12.4	-	11.4	-	11.9	-	12.0	-
P2*	Ag(111)	Ag$_3$	-	-	11.6	11 ± 1	11.6	-	11.8	-
	Cu(111)	Cu$_3$	-	-	11.3	-	11.3	11 ± 1	11.6	-
P3	Ag(111)	-	-	-	-	-	-	11 ± 1[19]	-	-
P3*	gas-phase	Ag$_1$	-	-	-	-	-	-	11.7	-

Energetics of HHTP-metal complexes.

In addition to theses geometrical considerations, we have carefully investigated the energetic behaviour of the different arrangements. Table 2 reports the calculated bonding energy per HHTP molecule and gives additional information on the role of the M_3 cluster (M = Cu, Ag) in the stabilization of the HHTP networks with different degrees of dehydrogenation. The gas phase P1 structure being always more stable than P2 at any degree of dehydrogenation (see Table 2), we expect to observe the P1 structure as long as adsorbed HHTP molecules respect the surface periodicity where HHTP-surface interactions are maximized, otherwise a mixture of P1 and P2 could be observed. This simple description is consistent with the experimental and calculated results reported in the present study. Note that on Au(111), which has a crystal structure close to that of Ag(111), both P1 and P2 structures are observed indifferently.[32] The interaction of HHTP with Cu_3 and Cu(111) is significantly stronger than with Ag_3 and Ag(111), in agreement with the higher reactivity of Cu(111). The presence of Ag_3 on the Ag(111) surface is highly beneficial to improve the stability of the HHTP network: the bonding energy increases by 1.06 eV/HHTP and 0.76 eV/HHTP on Ag_3/Ag(111) (P2*) relative to the sum of the individual Ag_3 (P2*) and Ag(111) (P2) components for the partially (-3H) and fully (-6H) dehydrogenation cases, respectively. The situation is slightly different for Cu where the gain in stability due to a bonding to Cu_3 for the partially (-3H) dehydrogenated HHTP network is relatively modest. The bonding energy of HHTP in Cu_3/Cu(111) (P2*) is larger than the sum of individual components by only 0.10 eV/HHTP. In contrast, the stability of the fully dehydrogenated HHTP system on Cu_3/Cu(111) (P2*) is clearly improved by 0.85 eV/HHTP with respect to the individual Cu_3 (P2*) and Cu(111) (P2) cases. Nevertheless, despite this significantly improved stability, Cu_3/Cu(111) (P2*) is rarely observed experimentally at high temperature of deposition. This surprising effect originates from the important structural reorganization required on Cu(111) and the incommensurability of (P2*) with the underlying surface. Our DFT calculations thus show that on Ag(111) the formation of P2* is energetically favorable and

13

structurally compatible, while on Cu(111) it is energetically even more favorable but structurally strongly unfavored. As a result, an extended P2* phase is observed on Ag(111) but only individual P2* motifs are allowed on Cu(111). Remarkably, the conclusions drawn here are robust against the dehydrogenation level, so the latter does not represent a crucial issue for the formation of HHTP metal-organic complexes.

Table 2: Calculated bonding energy[a] of HHTP assemblies (in eV/HHTP) where no, partial or total dehydrogenation have been considered.

system	surface	cluster	$(OH)_6$ dehydrogenation level			
			none (-0H)	partial (-2H)	partial (-3H)	full (-6H)
P1	gas-phase	-	0.46	0.77	0.47	0.33
	Ag(111)	-	1.02	2.23	-	-
P2	gas-phase		0.22	0.74	0.47	0.30
	Ag(111)	-	-	-	2.76	3.78
	Cu(111)	-	-	3.65	4.16	4.26[51]
P2*	gas-phase	Ag_3	0.52	1.86	1.20	1.29
	gas-phase	Cu_3	0.68	2.32	1.78	1.83
	Ag(111)	Ag_3	-	4.79	5.02	5.83
	Cu(111)	Cu_3	-	5.73	6.04	6.94
P3*	gas-phase	Ag_1	-	-	-	3.73

[a]Bonding energy is calculated according to E(complex)-E(M)-3*E(HHTP), where M may represent M_3, M(111) or M_3/M(111) with M = Ag, Cu, while HHTP can be the non, partially or fully dehydrogenated.

STM-imaging simulations of surface networks.

To support our description of the different phases and isolated structures observed, we have simulated STM images based on the Keldish-Green formalism of the different models after their structure has been optimized. Figure 3(a) shows the optimized balls-and-sticks models of the P1, P2 and P2* phases and the corresponding simulated STM images for HTTP/Ag(111), while the P2* structure on Cu(111) and the associated simulated STM images are presented in Figure 3(b). In the case of the Ag(111) surface, to compare DFT results to experimental data, we have modelled a molecular network, commensurate with the substrate through a (4×8) unit cell with a size of (11.61×23.22) Å^2. There are two

different types of molecules in this unit cell: one centred on top of a Ag atom of the substrate, and another one centred on a hcp hollow site of Ag(111). The simulated STM image (see Figure 3(a.1)) perfectly agrees with experimental STM data shown in Figure 1(a), with similar tunnelling bias conditions supporting the model proposed for the P1 arrangement. In the P2 phase, The molecular adlayer is perfectly commensurate with the substrate along a (4×4) supercell having a size of (11.64×11.64) $Å^2$. For this unit cell, there is a single type of HHTP molecule, that is on top of a Ag atom of the Ag(111) substrate. For the P2* phase on Ag(111), the on-surface Ag_3 ad-clusters stabilize the structure and favor the formation of a perfectly homogeneous metal-organic network by coordinating the molecules, with all the interfacial parameters similar to the case of P2. The simulated STM images with these two structural arrangements P2 and P2*, (Figure 3(a.3) and Figure 3(a.b) respectively, match the experimental observations (see Figure 1b), supporting our adsorption models.

We now describe the results of STM simulations obtained for the Cu(111) substrate. Since no clear commensuration/periodicity is experimentally detected for this structure, we have limited our STM simulations to three molecules surrounding one Cu_3 cluster, to reproduce the features observed in the experimental P2* structure (see Figure 1d). In addition, to understand the influence of -OH groups on the STM images, we have considered systems at different levels of dehydrogenation. Figure 3b shows two different optimized HTTP-Cu_3/Cu(111) interfacial models with partially dehydrogenated HHTP (Fig. 3b.1) and with fully-dehydrogenated HHTP molecules (Fig. 3b.2) While the last two models give rise to similar structural properties when considering the intermolecular distances (see Table 1), the height of the assembly over the surface is slightly smaller for the fully dehydrogenated case. The simulated STM images in Figure 3b (bottom panels) for fully dehydrogenated HHTP molecules show a good match with the experimental observations. Furthermore, we do not observe drastic variations of STM contrasts when going from partially to fully dehydrogenated systems. The agreement strongly justifies the proposed adsorption model
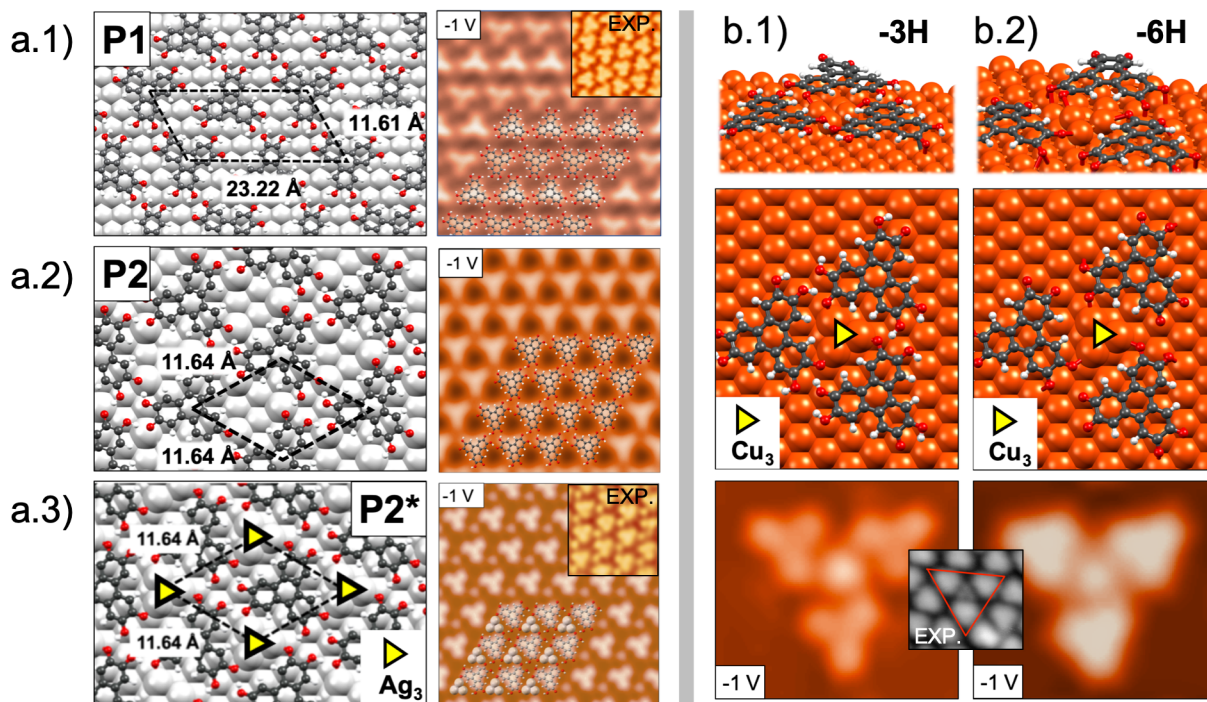
Figure 3: (a) Top view of the DFT-optimized interfacial structures for the P1 (a.1), P2 (a.2) and P2* (a.3) phases for HTTP/Ag(111) (left panels) and corresponding simulated STM images obtained at constant-current regime with I_t=0.1 nA and V_b=-1.0 V (right panels). (b) Perspective (top panels) and top (middle panels) views of three HTTP molecules coordinated by a Cu_3 on-surface ad-cluster for HHTP/Cu(111), and their associated simulated STM images (bottom panels) for partially (b.1) and fully-dehydrogenated (b.2) HHTP. The models white, grey, red, orange and silver spheres represent the H, C, O, Cu and Ag atoms, respectively. The molecular unit cell (indicating lattice parameters, a.1-3) used in the calculations is represented superimposed as a black dashed-lined box. Insets of experimental STM images from Fig. 1 are shown for comparison.

16

for P2* arrangement on Cu(111) surface.

Simulation of a metal-organic structure with single metal atoms.

Finally, we have investigated the formation of an additional P3* structure incorporating M1 metal atoms and forming a honeycomb network. Such 2D metal-organic framework (MOF) has been synthesized with Cu $(Cu_3(HHTP)_2)$[25] and has been recently used as cathodes in aqueous rechargeable zinc batteries.[26,27] Similar honeycomb network was reported in the literature on the Ag(111) surface after annealing at 500K, but the possible presence of metal adatoms was not raised.[19,29] While the participation of single metal substrate atoms to the formation of surface metal-organic frameworks is often assumed, their presence is not systematically revealed by STM,[14,56] and they are not clearly detected by XPS. DFT calculations are hence essential to support their existence. Here, we considered a hexagonal Ag-HHTP complex where fully dehydrogenated HHTP units are linked through a single Ag atom (P3* structure, see Figure 4). The calculated gas phase complex is highly stable (see Table 2), and the calculated distance between Ag atoms (L1 = 11.7 Å) in that complex is in excellent agreement with the periodicity (4×2.9 Å) of the Ag(111) surface. The calculated diameter of the hexagonal pore (L2 = 22.7 Å) is compatible with the experimental data reported previously for the high temperature P3 phase (22 ± 1 Å).[19,29] However, the experimental XPS data indicating partial dehydrogenation only[19] is in contradiction with the complete dehydrogenation of the hydroxyl groups that is required in such P3* metal-organic phase. Nevertheless, there is still the possibility that such a metal-organic structure forms locally as defects or small domains, especially when considering the observed non-homogeneity of the STM images.[29] The present result, supported by the strong influence of the crystal surface periodicity observed above for different metal-organic complexes, emphasizes the role of surface adatoms in the formation of surface complexes involving small metal clusters.
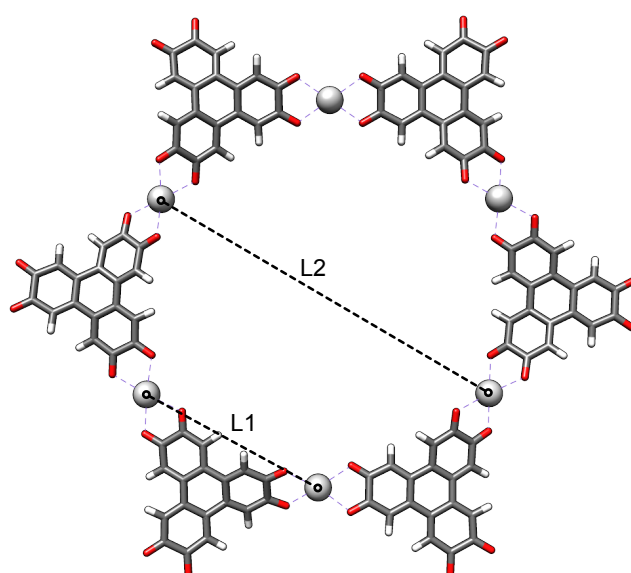
Figure 4: Optimized structure of the P3* (Ag-HHTP)$_6$ hexagonal complex where we identified the equilibrium distance between neighboring Ag atoms (L1 = 11.7 Å) and the diameter of the pore (L2 = 22.7 Å).

Conclusions

To summarize, we have combined experimental and theoretical efforts to investigate the formation of 2D metal-organic networks on Cu and Ag single-crystal surfaces. Our results indicate that the formation of extended metal-organic networks on surface strongly depends on the gain of stability in establishing metal-organic bonds, that is usually always positive, but more importantly on the structural compatibility of the 2D-MON formed with the atomic structure of the surface. Hence, we observed the formation of extended 2D-MON on Ag(111) where the presence of metal Ag clusters does not introduce drastic structural changes among the organic network and where the metal-organic bonds significantly improved the stability of the system. In other words, the Ag(111) surface presents the best structural/energetics synergy for HHTP to form extended metal-organic structures on the surface. In contrast, despite the higher reactivity of Cu and its great ability to form strong bonds with HHTP species, the structural changes induced by the presence of Cu clusters with the organic networks hinder the formation of an extended 2D-MON on Cu(111). In this work, we have demonstrated the major role of the atomic surface structure on the capability of forming extended metal-organic networks on surfaces.

A natural extension of our work could be a further theoretical exploration of the thermodynamics of the hybrid molecule / metal surface system. A thermochemical analysis, eventually delivering a stability phase diagram as a function of temperature and chemical potential, may indeed serve as a guide for the synthesis of specific on-surface molecular structures. Such an analysis would require to compute, starting from the energies we have calculated in the different structures we consider, the free energy of the system, and towards this, its temperature-dependent phononic response. While this is tractable for simpler on-surface systems, e.g. a well-defined surface oxide exposed to small molecules, with a relatively small unit cell onto a metal surface,[57] in the present case the more heterogeneous atomic distribution and large size of the molecules are computationally prohibitive. Alternative approaches are conceivable, for example based upon redox potential diagrams and

Einstein's model for vibrational modes.

Author Contributions

The manuscript was written through contributions of all authors.

Supporting Information

STM images: large scale network domains on Ag(111) and Cu(111); after annealing at 610K on Cu(111).

Notes

Conflicts of Interest: None

Acknowledgement

port from the "Région Nouvelle Aquitaine".

References

(1) Barth, J. V.; Costantini, G.; Kern, K. Engineering atomic and molecular nanostructures at surfaces. *Nature* **2005**, *437*, 671–679.

(2) Makoudi, Y.; Jeannoutot, J.; Palmino, F.; Chérioux, F.; Copie, G.; Krzeminski, C.; Cleri, F.; Grandidier, B. Supramolecular self-assembly on the B-Si(111)-($\sqrt{3}$x$\sqrt{3}$) R30° surface: From single molecules to multicomponent networks. *Surf. Sci. Rep.* **2017**, *72*, 316–349.

(3) Clair, S.; de Oteyza, D. G. Controlling a Chemical Coupling Reaction on a Surface: Tools and Strategies for On-Surface Synthesis. *Chem. Rev.* **2019**, *119*, 4717–4776.

(4) Mali, K. S.; Pearce, N.; De Feyter, S.; Champness, N. R. Frontiers of supramolecular chemistry at solid surfaces. *Chem. Soc. Rev.* **2017**, *46*, 2520–2542.

(5) Wan, X.; Liu, L.; Zhang, Y.; Liu, X.; Qian, Y.; Kan, E.; Kong, H.; Fuchs, H. Selective Construction of Magic Hierarchical Metal–Organic Clusters on Surfaces. *J. Phys. Chem. C* **2021**, *125*, 358–365.

(6) Hötger, D.; Carro, P.; Gutzler, R.; Wurster, B.; Chandrasekar, R.; Klyatskaya, S.; Ruben, M.; Salvarezza, R. C.; Kern, K.; Grumelli, D. Polymorphism and metal-induced structural transformation in 5,5'-bis(4-pyridyl)(2,2'-bispyrimidine) adlayers on Au(111). *Phys. Chem. Chem. Phys.* **2018**, *20*, 15960–15969.

(7) Fadeeva, A. I.; Gorbunov, V. A.; Stishenko, P. V.; Myshlyavtsev, A. V. Model of Fe-Terephthalate Ordering on Cu(100). *J. Phys. Chem. C* **2019**, *123*, 17265–17272.

(8) Čechal, J.; Kley, C. S.; Kumagai, T.; Schramm, F.; Ruben, M.; Stepanow, S.; Kern, K.

Functionalization of Open Two-Dimensional Metal–Organic Templates through the Selective Incorporation of Metal Atoms. *J. Phys. Chem. C* **2013**, *117*, 8871–8877.

(9) Clair, S.; Pons, S.; Fabris, S.; Baroni, S.; Brune, H.; Kern, K.; Barth, J. Monitoring two-dimensional coordination reactions: Directed assembly of Co-terephthalate nanosystems on Au(111). *J. Phys. Chem. B* **2006**, *110*, 5627–5632.

(10) Schlickum, U.; Decker, R.; Klappenberger, F.; Zoppellaro, G.; Klyatskaya, S.; Ruben, M.; Silanes, I.; Arnau, A.; Kern, K.; Brune, H. et al. Metal-Organic Honeycomb Nanomeshes with Tunable Cavity Size. *Nano Lett.* **2007**, *7*, 3813–3817.

(11) Stepanow, S.; Lingenfelder, M.; Dmitriev, A.; Spillmann, H.; Delvigne, E.; Lin, N.; Deng, X.; Cai, C.; Barth, J.; Kern, K. Steering molecular organization and host-guest interactions using two-dimensional nanoporous coordination systems. *Nature Mater.* **2004**, *3*, 229–233.

(12) Han, Y.; Wang, J.; Song, L.; Zheng, Y.; Li, Y.; Lin, H.; Li, Q.; Chi, L. A Fundamental Role of the Molecular Length in Forming Metal–Organic Hybrids of Phenol Derivatives on Silver Surfaces. *J. Phys. Chem. Lett.* **2021**, *12*, 1869–1875.

(13) Barth, J. V. Fresh perspectives for surface coordination chemistry. *Surf. Sci.* **2009**, *603*, 1533 – 1541.

(14) Dong, L.; Gao, Z.; Lin, N. Self-assembly of metal–organic coordination structures on surfaces. *Prog. Surf. Sci.* **2016**, *91*, 101–135.

(15) Bebensee, F.; Bombis, C.; Vadapoo, S.-R.; Cramer, J. R.; Besenbacher, F.; Gothelf, K. V.; Linderoth, T. R. On-Surface Azide–Alkyne Cycloaddition on Cu(111): Does It "Click" in Ultrahigh Vacuum? *J. Am. Chem. Soc.* **2013**, *135*, 2136–2139.

(16) Lo Cicero, M.; Della Pia, A.; Riello, M.; Colazzo, L.; Sedona, F.; Betti, M. G.; Sambi, M.; De Vita, A.; Mariani, C. A long-range ordered array of copper tetrameric

units embedded in an on-surface metal organic framework. *J. Chem. Phys.* **2017**, *147*, 214706.

(17) Ruiz del Árbol, N.; Palacio, I.; Otero-Irurueta, G.; Martínez, J. I.; de Andrés, P. L.; Stetsovych, O.; Moro-Lagares, M.; Mutombo, P.; Svec, M.; Jelínek, P. et al. On-Surface Bottom-Up Synthesis of Azine Derivatives Displaying Strong Acceptor Behavior. *Angew. Chem. Int. Ed.* **2018**, *130*, 8718–8722.

(18) Gómez-Herrero, A. C.; Sánchez-Sánchez, C.; Chérioux, F.; Martínez, J. I.; Abad, J.; Floreano, L.; Verdini, A.; Cossaro, A.; Mazaleyrat, E.; Guisset, V. et al. Copper-assisted oxidation of catechols into quinone derivatives. *Chem. Sci.* **2021**, *12*, 2257–2267.

(19) Giovanelli, L.; Ourdjini, O.; Abel, M.; Pawlak, R.; Fujii, J.; Porte, L.; Themlin, J.-M.; Clair, S. Combined Photoemission Spectroscopy and Scanning Tunneling Microscopy Study of the Sequential Dehydrogenation of Hexahydroxytriphenylene on Ag(111). *J. Phys. Chem. C* **2014**, *118*, 14899–14904.

(20) Svane, K. L.; Baviloliaei, M. S.; Hammer, B.; Diekhöner, L. An extended chiral surface coordination network based on Ag7-clusters. *J. Chem. Phys.* **2018**, *149*, 164710.

(21) Liu, J.; Fu, X.; Chen, Q.; Zhang, Y.; Wang, Y.; Zhao, D.; Chen, W.; Xu, G. Q.; Liao, P.; Wu, K. Stabilizing surface Ag adatoms into tunable single atom arrays by terminal alkyne assembly. *Chem. Commun.* **2016**, *52*, 12944–12947.

(22) Knecht, P.; Suryadevara, N.; Zhang, B.; Reichert, J.; Ruben, M.; Barth, J. V.; Klyatskaya, S.; Papageorgiou, A. C. The self-assembly and metal adatom coordination of a linear bis-tetrazole ligand on Ag(111). *Chem. Commun.* **2018**, *54*, 10072–10075.

(23) Hua, M.; Xia, B.; Wang, M.; Li, E.; Liu, J.; Wu, T.; Wang, Y.; Li, R.; Ding, H.; Hu, J. et al. Highly Degenerate Ground States in a Frustrated Antiferromagnetic Kagome Lattice in a Two-Dimensional Metal–Organic Framework. *J. Phys. Chem. Lett.* **2021**, *12*, 3733–3739.
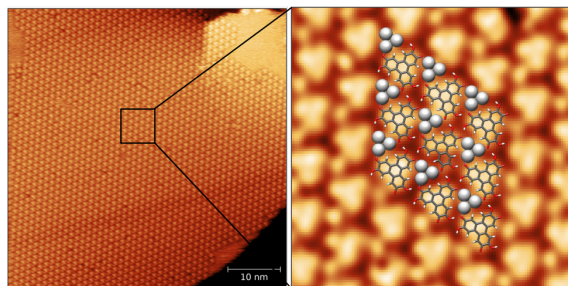
(24) Robles, R.; Zobač, V.; Au Yeung, K. H.; Moresco, F.; Joachim, C.; Lorente, N. Supramolecular chemistry based on 4-acetylbiphenyl on Au(111). *Phys. Chem. Chem. Phys.* **2020**, *22*, 15208–15213.

(25) Hmadeh, M.; Lu, Z.; Liu, Z.; Gándara, F.; Furukawa, H.; Wan, S.; Augustyn, V.; Chang, R.; Liao, L.; Zhou, F. et al. New Porous Crystals of Extended Metal-Catecholates. *Chem. Mater.* **2012**, *24*, 3511–3513.

(26) Sonet, D.; Bibal, B. Triphenylene: A versatile molecular receptor. *Tetrahedron Lett.* **2019**, *60*, 872 – 884.

(27) Nam, K. W.; Park, S. S.; dos Reis, R.; Dravid, V. P.; Kim, H.; Mirkin, C. A.; Stoddart, J. F. Conductive 2D metal-organic framework for high-performance cathodes in aqueous rechargeable zinc batteries. *Nature Commun.* **2019**, *10*, 4948.

(28) Morshedi, M.; Willis, A. C.; White, N. G. Anion-templated 2D frameworks from hexahydroxytriphenylene. *Cryst. Eng. Comm.* **2016**, *18*, 4281–4284.

(29) Pawlak, R.; Clair, S.; Oison, V.; Abel, M.; Ourdjini, O.; Zwaneveld, N. A. A.; Gigmes, D.; Bertin, D.; Nony, L.; Porte, L. Robust Supramolecular Network on Ag(111): Hydrogen-Bond Enhancement through Partial Alcohol Dehydrogenation. *Chem. Phys. Chem* **2009**, *10*, 1032–1035.

(30) Clair, S.; Abel, M.; Porte, L. Mesoscopic Arrays from Supramolecular Self-Assembly. *Angew. Chem. Int. Ed.* **2010**, *49*, 8237–8239.

(31) Coratger, R.; Calmettes, B.; Abel, M.; Porte, L. STM observations of the first polymerization steps between hexahydroxy-tri-phenylene and benzene-di-boronic acid molecules. *Surf. Sci.* **2011**, *605*, 831–837.

(32) Marele, A. C.; Corral, I.; Sanz, P.; Mas-Ballesté, R.; Zamora, F.; Yáñez, M.; Gómez-Rodríguez, J. M. Some Pictures of Alcoholic Dancing: From Simple to Complex

Hydrogen-Bonded Networks Based on Polyalcohols. *J. Phys. Chem. C* **2013**, *117*, 4680–4690.

(33) Horcas, I.; Fernández, R.; Gómez-Rodríguez, J. M.; Colchero, J.; Gómez-Herrero, J.; Baro, A. M. WSXM: A software for scanning probe microscopy and a tool for nanotechnology. *Rev. Sci. Instrum.* **2007**, *78*, 013705.

(34) Nečas, D.; Klapetek, P. Gwyddion: an open-source software for SPM data analysis. *Open Phys.* **2012**, *10*, 181–188.

(35) Valiev, M.; Bylaska, E. J.; Govind, N.; Kowalski, K.; Straatsma, T. P.; Van Dam, H. J. J.; Wang, D.; Nieplocha, J.; Apra, E.; Windus, T. L. et al. NWChem: A comprehensive and scalable open-source solution for large scale molecular simulations. *Comput. Phys. Comm.* **2010**, *181*, 1477–1489.

(36) Adamo, C.; Barone, V. Toward reliable density functional methods without adjustable parameters: The PBE0 model. *J. Chem. Phys.* **1999**, *110*, 6158–6170.

(37) Grimme, S. Semiempirical GGA-type density functional constructed with a long-range dispersion correction. *J. Comput. Chem.* **2006**, *27*.

(38) Giannozzi, P.; Baroni, S.; Bonini, N.; Calandra, M.; Car, R.; Cavazzoni, C.; Ceresoli, D.; Chiarotti, G. L.; Cococcioni, M.; Dabo, I. et al. QUANTUM ESPRESSO: a modular and open-source software project for quantum simulations of materials. *J. Condens. Matter Phys.* **2009**, *21*, 395502.

(39) Perdew, J. P.; Burke, K.; Ernzerhof, M. Generalized Gradient Approximation Made Simple. *Phys. Rev. Lett.* **1996**, *77*, 3865–3868.

(40) Rappe, A. M.; Rabe, K. M.; Kaxiras, E.; Joannopoulos, J. D. Optimized pseudopotentials. *Phys. Rev. B* **1990**, *41*, 1227–1230.

(41) Mounet, N.; Marzari, N. First-principles determination of the structural, vibrational and thermodynamic properties of diamond, graphite, and derivatives. *Phys. Rev. B* **2005**, *71*, 205214.

(42) Pack, J. D.; Monkhorst, H. J. "Special points for Brillouin-zone integrations"—a reply. *Phys. Rev. B* **1977**, *16*, 1748–1749.

(43) Blanco, J. M.; González, C.; Jelínek, P.; Ortega, J.; Flores, F.; Pérez, R. First-principles simulations of STM images: From tunneling to the contact regime. *Phys. Rev. B* **2004**, *70*, 085405.

(44) Lewis, J. P.; Jelínek, P.; Ortega, J.; Demkov, A. A.; Trabada, D. G.; Haycock, B.; Wang, H.; Adams, G.; Tomfohr, J. K.; Abad, E. et al. Advances and applications in the FIREBALL ab initio tight-binding molecular-dynamics formalism. *Phys. Status Solidi (b)* **2011**, *248*, 1989–2007.

(45) Tersoff J.,; Hamann D. R., Theory of scanning tunneling microscope. *Phys. Rev. B* **1985**, *31*, 805.

(46) Oikawa, S.; Hirosawa, I.; Hirakawa, K.; Kawanishi, S. Site specificity and mechanism of oxidative DNA damage induced by carcinogenic catechol. *Carcinogenesis* **2001**, *22*, 1239–1245.

(47) Hirakawa, K.; Oikawa, S.; Hiraku, Y.; Hirosawa, I.; Kawanishi, S. Catechol and Hydroquinone Have Different Redox Properties Responsible for Their Differential DNA-damaging Ability. *Chem. Res. Toxicol.* **2002**, *15*, 76–82.

(48) Guo, L.; Sun, J.; Zhang, W.; Hou, L.; Liang, L.; Liu, Y.; Yuan, C. Bottom-Up Fabrication of 1D Cu-based Conductive Metal–Organic Framework Nanowires as a High-Rate Anode towards Efficient Lithium Storage. *Chem. Sus. Chem.* **2019**, *12*, 5051–5058.

(49) Meng, X.; Kolodzeiski, E.; Huang, X.; Timmer, A.; Schulze Lammers, B.; Gao, H.-Y.; Mönig, H.; Liu, L.; Xu, W.; Amirjalayer, S. et al. Tunable Thiolate Coordination Networks on Metal Surfaces. *Chem. Nano Mat.* **2020**, *6*, 1479–1484.

(50) Svane, K. L.; Linderoth, T. R.; Hammer, B. Structure and role of metal clusters in a metal-organic coordination network determined by density functional theory. *J. Chem. Phys.* **2016**, *144*, 084708.

(51) Gómez-Herrero, A. C. Towards tow-dimensional organo-metallic molecular architectures via interface chemistry. Ph.D. thesis, Univ. Grenoble Alpes, 2019.

(52) Matena, M.; Björk, J.; Wahl, M.; Lee, T.-L.; Zegenhagen, J.; Gade, L. H.; Jung, T. A.; Persson, M.; Stöhr, M. On-surface synthesis of a two-dimensional porous coordination network: Unraveling adsorbate interactions. *Physical Review B* **2014**, *90*, 125408.

(53) Bebensee, F.; Svane, K.; Bombis, C.; Masini, F.; Klyatskaya, S.; Besenbacher, F.; Ruben, M.; Hammer, B.; Linderoth, T. R. A Surface Coordination Network Based on Copper Adatom Trimers. *Angewandte Chemie International Edition* **2014**, *53*, 12955–12959.

(54) Martin-Gondre, L.; Bocan, G. A.; Blanco-Rey, M.; Alducin, M.; Juaristi, J. I.; Díez Muiño, R. Scattering of Nitrogen Atoms off Ag(111) Surfaces: A Theoretical Study. *J. Phys. Chem. C* **2013**, *117*, 9779–9790.

(55) Tafreshi, S. S.; Roldan, A.; de Leeuw, N. H. Density Functional Theory Study of the Adsorption of Hydrazine on the Perfect and Defective Copper (100), (110), and (111) Surfaces. *J. Phys. Chem. C* **2014**, *118*, 26103–26114.

(56) Lin, N.; Barth, J. V. Surface-Confined Supramolecular Coordination Chemistry. *Top. Curr. Chem.* **2009**, *287*, 1–44.

(57) Reuter, K.; Scheffler, M. Composition, structure, and stability of RuO_2(110) as a function of oxygen pressure. *Phys. Rev. B* **2001**, *65*, 035406.

TOC Graphic